Journal of Hydraulic Structures
***J. Hydraul. Struct.*, 2018; 4(2):27-41**
DOI: 10.22055/JHS.2018.27848.1093

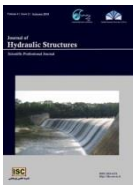

OPEN ACCESS

Characteristic Based Split Finite Element for Unsteady Dam-Break Problem

Javad Parsa[1]

Abstract

In this paper, an efficient numerical model for solution of the two-dimensional unsteady dam-break problem is described. The model solves the shallow water equations through Characteristic-Based Split (CBS) finite element method. The formulation of the model is based upon the fractional time step technique primarily used in the finite difference method for the incompressible Navier-Stokes equations. In addition to well-known advantages of the finite element discretization in introducing complex geometries and making accurate results near the boundaries, the CBS utilizes interesting advantages. These include the ability of the method to simulate both compressible and incompressible flows using the same formulation. Improved stability of the CBS algorithm along with its capability to simulate both sub- and super-critical flows are other main advantages of the method. These useful advantages of the algorithm introduce the CBS as a unique procedure to solve fluid dynamics problems under various conditions. Since dam-break problem has principally a high non-linear nature, the model is verified firstly by modeling one-dimensional problems of dam-break and bore formation problems. Furthermore, application of the model to a two-dimensional hypothetical dam-break problem shows the robustness and efficiency of the procedure. Despite the high non-linearity nature of the solved problems, the computational results, compared with the analytical solutions and reported results of other numerical models, indicate the favorable performance of the used procedure in modeling the dam-break problems.

Keywords: Characteristic-Based Split finite element, shallow water, dam-break, bore.

Received: 9 December 2018; Accepted: 25 December 2018

1. Introduction

The computation of unsteady flows is required for the prediction of flood waves in rivers, flows generated by failure of dams and flow conditions in the vicinity of hydraulic structures [1-3]. Numerical models have been introduced as suitable alternatives to other form of flow simulations such as experimental studies [4,5]. Indeed, numerical models have utilized as an essential predictive tool to assess the risks associated with the failure of the hydraulic structures [5,6]. In the recent

[1] Water Engineering Department, Faculty of Agriculture, University of Tabriz, Tabriz, Iran, jparsa@tabrizu.ac.ir (**Corresponding author**)

decades, one-dimensional numerical models have been extensively used to simulate the unsteady dam-break problem. Relatively accurate description of the dam-break problem in real situations needs to use two-dimensional models [7,8]. Accuracy of the dam-break simulation results from these models is adequate for engineering applications. Modeling of two-dimensional unsteady flow during breaking a dam is more complicated than one-dimensional one because of need for efficient solver routines and the inclusions of suitable boundary conditions. Complexity of these computations is mainly due to occurrence of both sub-critical and super-critical flows after breaking a dam.

Shallow water equations are non-linear first-order hyperbolic partial differential equations. The hyperbolic nature of these equations creates remarkable difficulties in the numerical solutions. The solutions of this type of equations obtained by numerical procedures are often discontinuous regardless of whether the initial conditions are smooth or highly fluctuating [9]. Since the equations have the non-linear character, their analytical solutions are possible in very simplified one-dimensional situations and therefore, these equations are to be solved numerically for practical problems.

Numerical experiments, however, show that most of numerical procedures fail if high non-linearity occurs in the flow field. For instance, it is well-known that simple and direct finite element forms usually fail for shallow water problems due to instability which results in sever oscillations of the solution [10]. Similar to making use of stabilizers in the finite difference context, stabilization procedures have been introduced into some finite element formulations permitting the use the original discretization schemes. The Characteristic-Based Split, hereafter also denoted as CBS, algorithm is one of the most suitable finite element based numerical techniques for shallow water equations that utilizes the stabilization mechanism. This method utilizes both advantages of characteristics method for hyperbolic partial differential equations and nodaly exact results of Galerkin weighted residual method for self-adjoint problems.

The Characteristic-Based Split algorithm and its interesting advantages are presented in detail in many earlier studies [10-22]. Here, a brief summary on the algorithm is given. The CBS algorithm is based on the original Chorin split [23] and also has similarities with the projection method widely used in compressible flow modeling. Based upon the Chorin technique, the discretization of the equations in the time advancement consists of two or more steps. The numerical behavior of the equations is affected using this splitting technique and the simpler sub-problems are achieved [14]. The velocity correction step is the key point in the CBS algorithm. The CBS algorithm makes use of Galerkin method along the characteristics for advection-dominated problems with a velocity correction stage. Using Characteristic-Galerkin procedure, the velocities are computed in two steps. Firstly, an intermediate velocity field is computed after elimination of the pressure type terms from the momentum equations. The pressure is obtained in the next step by solving the continuity equation that utilizes the intermediate velocity field determined in the previous step. A Laplacian form of the continuity equation is used making the use of Galerkin space discretization optimal. In the final step, the computed pressure type term is used to modify the velocity field. Some remarkable advantages of the algorithm for modeling of shallow water problems can be summarized as follows. Firstly, the stability of the algorithm is on the basis of the current velocity rather than the wave celerity leading to more stability of the method. Secondly, the standard Galerkin procedure is applied along the characteristics because of the splitting of the pressure type terms. The use of Characteristic-based Galerkin discretization and splitting of the pressure type terms, have made the CBS algorithm a unified approach to deal with both compressible and incompressible fluid flows and sub-critical and super-critical flows in water engineering problems, as well [16,17].

This paper presents the formulation of the Characteristic-Based Split finite element method for

the shallow water equations and its application to the simulation of the dam failure and bore formation. The Characteristic-Based Split finite element method has been never applied for dam break problem, especially for two-dimensional dam break.

The rest of the paper is structured as follows. The shallow water equations are reviewed in the first section. This is followed by the finite element formulation making use of the Characteristic-Based Split method. Numerical examples including two one-dimensional examples of a bore formation and a dam-break problem and a two-dimensional dam-break problem are discussed in the fourth section. The paper concludes with the concluding remarks in the last section.

2. Mathematical model

Modeling flow hydrodynamics in shallow water bodies requires the prediction of water depth and depth integrated velocities in both x and y directions. In the derivation of shallow water equations from Navier-Stokes equations, some assumptions are necessary. The constant density of fluid, hydrostatic pressure distribution and making use of suitable free surface and boundary conditions are of the assumptions required for derivation of shallow water equations [6]. A schematic figure of the basic situation is shown in Figure 1.

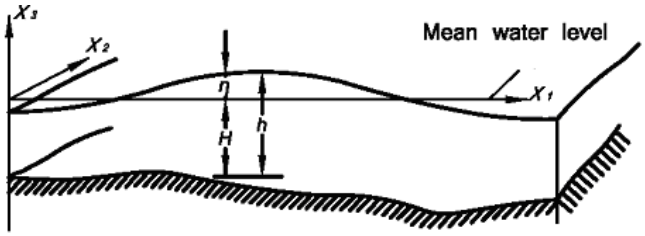

Figure 1. Schematic representation of the geometric setting.

The conservative form of the shallow water equations in Cartesian coordinate system can be written as [16,17,22]:

$$\frac{\partial h}{\partial t}+\frac{\partial U_i}{\partial x_i}=0 \tag{1}$$

$$\frac{\partial U_i}{\partial t}+\frac{\partial F_{ij}}{\partial x_j}+\frac{\partial p}{\partial x_i}+S_i=0 \tag{2}$$

where i, j =1, 2, the vector of U is $U_i = hu_i$, h is the water depth, u_i is the i^{th} component of the averaged velocity over the depth; F_{ij} is the i^{th} component of the j flux vector and the pressure type term p is given by:

$$p=\frac{1}{2}g\left(h^2-H^2\right) \tag{3}$$

where H is the bathymetry elevation measured with respect to an arbitrary horizontal reference level. As shown in Figure 1, the water depth , h, is the water surface elevation with respect to the bathymetry and can be computed by $h = H + \eta$. The variable η denotes the free surface elevation in regard to an arbitrary horizontal reference level. Finally, S_i is the i^{th} component of a source vector, which can be expressed as:

$$S_i = -g(h-H)\frac{\partial H}{\partial x_i} + g\frac{n^2 u_i|u|}{h^{\frac{4}{3}}} + r_i - \tau_i \tag{4}$$

The source terms in equation (4) are obtained by depth integration. The terms in this equation include the slope of bottom, the friction of bottom (Manning formula), the force of Coriolis and wind tractions τ_i. Here $r_i = -f U_j$ where f denotes the Coriolis factor.

3. Numerical model

Using the concept of characteristics in temporal discretization of the shallow water equations, equations (1) and (2), arrived at the following equations [16]:

$$\left(\frac{1}{c^2}\right)^n \Delta p = -\Delta t\left[\frac{\partial U_i^n}{\partial x_i} + \theta_1 \frac{\partial(\Delta U_i)}{\partial x_i}\right] \tag{5}$$

$$\Delta U_i = -\Delta t\left[\frac{\partial F_{ij}}{\partial x_j} + S_i\right]^n + \frac{\Delta t^2}{2}\left[u_k \frac{\partial}{\partial x_k}\left(\frac{\partial F_{ij}}{\partial x_j} + S_i\right)\right]^n - \Delta t \frac{\partial p^{n+\theta_2}}{\partial x_i} \tag{6}$$

in which:

$$\frac{\partial p^{n+\theta_2}}{\partial x_i} = (1-\theta_2)\frac{\partial p^n}{\partial x_i} + \theta_2 \frac{\partial p^{n+1}}{\partial x_i} - (1-\theta_2)\frac{\Delta t}{2} u_k \frac{\partial}{\partial x_k}\left(\frac{\partial p^n}{\partial x_i}\right) \tag{7}$$

where ($0 \le \theta_1, \theta_2 \le 1$), ($k$ =1, 2), the incremental variables Δp and ΔU_i are the increments of the variables over a time step Δt and c ,the long waves celerity, is related to p with the depth of water by:

$$c^2 = \frac{dp}{dh} = gh \tag{8}$$

The method is completed by omitting ΔU_i in the equation (5) by computing the divergence of equation (6) and replacing the obtained equations into equation (5). The following 'self-adjoint' type equation for the variable p is resulted in:

$$\frac{1}{c^2}\frac{\Delta p}{\Delta t} - \theta_1\theta_2 \frac{\partial}{\partial x_i}\frac{\partial(\Delta p)}{\partial x_i} = -\frac{\partial}{\partial x_i}\left(U_i^n + \theta_1 \Delta U_i^*\right) + \theta_1 \Delta t \frac{\partial}{\partial x_i}\frac{\partial p^n}{\partial x_i} \tag{9}$$

The 'intermediate' variable ΔU_i^* computed explicitly. It denotes the first two terms in square brackets of equation (6). Calculation of the pressure type variable and the depth averaged velocity at the time (n + 1)Δt, p^{n+1} and U_i^{n+1}, is conducted through the following steps: first, the intermediate variable ΔU_i^* is computed, then the incremental pressure term Δp is calculated and at the final step, the intermediate velocities are corrected to attain the final velocity values, i.e. the complete momentum equation (6). The equations (6), (7) and (9) are performing the time discretization along the characteristics. A backward approximate integration gives the mentioned equations with extra convection stabilizers (the second bracket terms in right-hand side of equation (6)). These stabilization terms are consistent and extirpate the oscillations due to highly convective flows [10].

3.1. Spatial discretization

The spatial discretization of the equations obtained during the mentioned three steps is stated here. The first two terms on the right-hand side of equation (6) are discretized using the Gauss–Green theorem and the standard Galerkin technique as follows:

$$\begin{aligned}\int_\Omega N_u^l \Delta U_i^* d\Omega = \Delta t \Bigg[& -\int_\Omega N_u^l \frac{\partial F_{ij}}{\partial x_j} d\Omega - \int_\Omega N_u^l (S_i) d\Omega \\ & - \frac{\Delta t}{2} \int_\Omega \frac{\partial}{\partial x_k} \left(N_u^l u_k \right) \frac{\partial F_{ij}}{\partial x_j} d\Omega + \frac{\Delta t}{2} \int_\Omega N_u^l u_k \frac{\partial (S_i)}{\partial x_k} d\Omega \\ & + \frac{\Delta t}{2} \int_\Gamma N_u^l u_k \frac{\partial F_{ij}}{\partial x_j} n_k d\Gamma \Bigg]^n \end{aligned} \tag{10}$$

in which Ω denotes the solution domain bounded by Γ, N_u^l and N_r^l represent the standard weighting function for U and S in node l and n_k is the k^{th} component of the outward normal vector of the boundary of computational domain. The right-hand side of equation (10) is computed at time t^n.

Making use of the wave celerity definition in equation (8), the pressure type term is computed in terms of h. The standard Galerkin technique along with the Gauss–Green theorem are applied to equation (9) and the following discretized equation results:

$$\begin{aligned}\int_\Omega N_h^l \Delta h d\Omega + \theta_1 \theta_2 \Delta t^2 \int_\Omega \frac{\partial N_h^l}{\partial x_i} \hat{c}^2 \frac{\partial (\Delta h)}{\partial x_i} d\Omega = \\ - \Delta t \int_\Omega N_u^l \frac{\partial U_i^n}{\partial x_j} d\Omega + \theta_1 \Delta t \int_\Omega \frac{\partial N_u^l}{\partial x_i} \Delta U_i^* d\Omega \\ - \theta_1 \Delta t^2 \int_\Omega \frac{\partial N_h^l}{\partial x_i} \left(c^2 \right)^n \frac{\partial h^n}{\partial x_i} d\Omega \\ - \theta_1 \Delta t \int_\Gamma N_u^l \Delta U_i^* n_i d\Gamma \\ + \theta_1 \Delta t^2 \int_\Gamma N_h^l \left(\left(c^2 \right)^n \frac{\partial h^n}{\partial x_i} + \theta_2 \hat{c}^2 \frac{\partial (\Delta h)}{\partial x_i} \right) n_i d\Gamma \end{aligned} \tag{11}$$

in which $\hat{c}$ is the averaged wave celerity over the time step Δt and $(c^2)^n$ is calculated at time t^n. The velocity field correction as the final step, is written by considering equation (6). After making use of Galerkin procedure and some appropriate manipulations of the second-order term of equation (6), its spatial discretized form becomes as:

$$\int_\Omega N_u^l \Delta U_i \, d\Omega = \Delta t \int_\Omega N_u^l \frac{\Delta U_i^*}{\Delta t} d\Omega - (1-\theta_2)\Delta t \int_\Omega N_h^l \left(c^2\right)^n \frac{\partial h^n}{\partial x_i} d\Omega$$
$$- \theta_2 \Delta t \int_\Omega N_h^l \left(c^2\right)^{n+1} \frac{\partial h^{n+1}}{\partial x_i} d\Omega$$
$$- (1-\theta_2)\frac{\Delta t^2}{2} \int_\Omega \frac{\partial N_h^l}{\partial x_k} u_k \left(\left(c^2\right)^n \frac{\partial h^n}{\partial x_i} \right) d\Omega \qquad (12)$$
$$- (1-\theta_2)\frac{\Delta t^2}{2} \int_\Omega N_h^l \frac{\partial u_k}{\partial x_k} \left(\left(c^2\right)^n \frac{\partial h^n}{\partial x_i} \right) d\Omega$$
$$+ (1-\theta_2)\frac{\Delta t^2}{2} \int_\Gamma N_h^l u_k \left(\left(c^2\right)^n \frac{\partial h^n}{\partial x_i} \right) d\Gamma$$

3.2. Boundary conditions

Several boundary conditions of different types and their implementations have been described in many references, e.g. [17,21,25-30]. The implementation of the boundary conditions in the methodology of CBS is similar to that in other schemes. To implement the boundary conditions in the methodology of CBS, no special conditions are imposed for the computation of the ΔU_i^*. In equation (11) two last terms are the normal components of momentum which are computed of order Δt. The velocity components normal to the wall and open boundaries are defined by modifying step for these type of boundary conditions [16,17,21].

3.3. Final discrete form and time integration

The following steps are performed to arrive at the final form of numerical procedure [8]:

i. *Computation of the intermediate variable*: The following spatial approximations are used in equation (10) for this step:

$$U_i^n = N_u^l . U_i^{l(n)}$$
$$\Delta U_i^* = N_u^l . \Delta U_i^{*l}$$
$$h^n = N_h^l . h^{l(n)} \qquad (13)$$
$$H = N_h^l . H^l$$

ii. *Pressure computation step*: The calculation of *h* is carried out using equation (17) and based on the following spatial discretization:

$$
\begin{aligned}
h^n &= N_h^l . h^{l(n)} \\
\Delta h &= N_h^l . \Delta h^l \\
U_i^n &= N_u^l . U_i^{l(n)} \\
\Delta r &= N_u^l . \Delta r^l
\end{aligned}
\tag{14}
$$

iii. *Momentum correction step*: The correction is established by equation (12) and the following approximations are used to equation (12) to carry out the correction of the momentum of flow:

$$
\begin{aligned}
h^n &= N_h^l . h^{l(n)} \\
h^{n+1} &= N_h^l . h^{l(n+1)} \\
\Delta U_i^n &= N_u^l . \Delta U_i^l \\
\Delta U_i^* &= N_u^l . \Delta U_i^{*l}
\end{aligned}
\tag{15}
$$

The stability of computation of ΔU_i^* is conditional. The simplified stability criterion in one-dimensional state can be represented by $\Delta t_{crit} \le \varepsilon L / |u|$, where L is the smallest dimension of element and the values of ε for consistent and lumped mass matrices are 1/3 and 1, respectively. The second and third steps of the method can be computed explicitly or semi-implicitly based on the chosen values for θ_1 and θ_2. For the fully explicit solution ($\theta_2 = 0$), the limit of stability finds equal to the explicit solutions and the procedure will be similar to the Taylor–Galerkin method [17,21]. When a semi-implicit solution is chosen ($0.5 \le \theta_1 \le 1$ and $0.5 \le \theta_2 \le 1$), the limit of stability for the defined CBS procedure is characterized by the computation of intermediate momentum.

4. Results and discussion

The performance of the described algorithm on shallow water problems is evaluated by some numerical experiments. To achieve this aim, the following benchmark problems are solved in this paper. In these problems, the uniform meshes which include the triangular linear elements are used.

In what follows, two set of problems are given. The first set deals with the flows in pseudo-one-dimensional situation. The second set is two-dimensional one. These problems include the formation of shock waves by advancing the solution which are good tests for demonstraiting the capability of the scheme in modeling the severe natural hydraulic problems.

4.1. One-dimensional problems

As the first application of the described scheme, the classical Stoker test case is studied. In this case, the one-dimensional breaking of a dam over a wet bed is considered. Stoker's exact solution [29] to the one-dimensional dam break is the superimposition of up-going rarefaction and down-going shock waves connected by a middle zone with a constant depth and a constant velocity (see, e.g., [31]). To execute this test, a dam lies at the middle of a rectangular flat channel and it is assumed that the dam fails instaneously. Because of discontinues initial

conditions and transition of flow from sub-critical to super-critical, it represents a severe test which has highlighted problems with a number of numerical schemes. The computational domain comprises of a 100×1 m^2. The water is initially at rest in the reservoir and tillage and the initial water depths are:

$$h(x,0)=\begin{cases}2\ m & if\ \ x<50\ m\\ 1\ m & if\ \ x\geq 50\ m\end{cases} \tag{16}$$

The gravity acceleration is assumed to be g = 9.8 m/sec^2. The discretized domain involves 100×8 triangular linear elements having same sizes. Suddenly, the dam removed and the computation of flow over the whole domain started using Δt = 0.1 *sec*.

The obtained results for water surface elevations and longitudinal velocities along the entire domain after collapsing the dam for 2.5 sec, 5 sec and 7.5 sec are shown in Figures 2 and 3 and they are compared favorably with analytical solution reported in [29]. As shown in these figures, the numerical results agree very well with those from analytical solutions. It is clear that the flow velocities and shock wave fronts advancing in downstream have been modeled accurately. Compared with the exact solution, overshoots occurs around the shock wave, together with an oscillation close to the rarefaction wave. The wave front clearly agree with the exact solution, and the main differences between the exact solution and the numerical results are localized just close to the discontinuities.

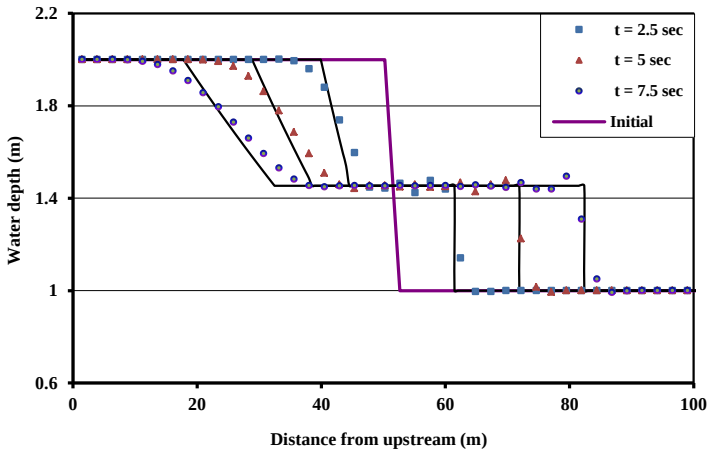

Figure 2. Comparison of the model results with the analytical solution for dam break problem.

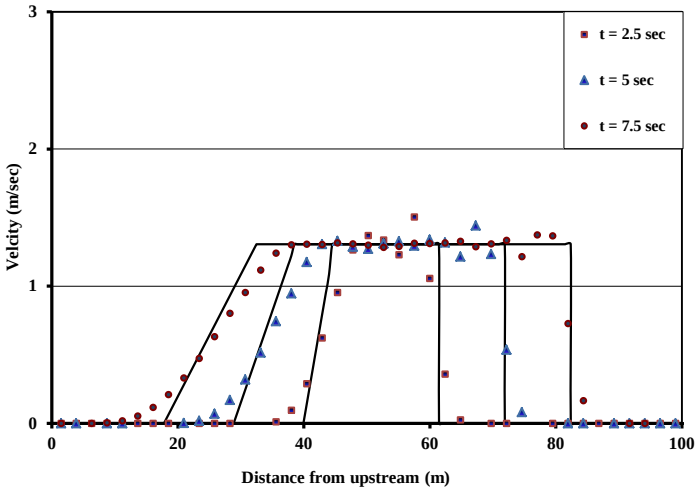

Figure 3. Longitudinal velocities along the entire domain compared with the analytical solution.

The problem of bore formation and propagation along a rectangular flat channel is the second test studied here. The depth of 1 m and velocity of 1 m/sec along the entire channel are given as the initial conditions. Boundary conditions are imposed as the flow velocity of 1 m/sec in the upstream and a sinusoidal rising water elevation with period of 120 sec in the downstream boundary of the channel. After t = 30 sec the total water depth is imposed as 3 m at this boundary. This situation illustrates that a bore forms and then propagates in upstream direction. In order to solve the problem, a rectangular flat channel with the length of 200 m and width of 1 m is considered. The whole domain decomposes to 200×8 triangular elements and the model is executed using time step Δt = 0.1 sec. The results obtained for water surface profiles and velocities during the bore propagation are shown in Figures 4 and 5. As seen, the wave fronts are well modeled and very small oscillations just occur close to the discontinuities. Comparison of the results shown in Figures 4 and 5 with those of reported in literature, e.g. [22], indicates that they have been employed coarser meshes to avoid the oscillations while the shocks were modeled milder. It is a common practice that the accurate modeling of a shock always produces some oscillations in its vicinity due to the omitting of higher order terms in the discretization process of the governing equations. In the other words, the steeper shock, the more oscillatory solution. However, the obtained results are well comparable with those of reported in [22]. The superiority of the CBS technique is its ability to model the shocks accurately with less oscillation.

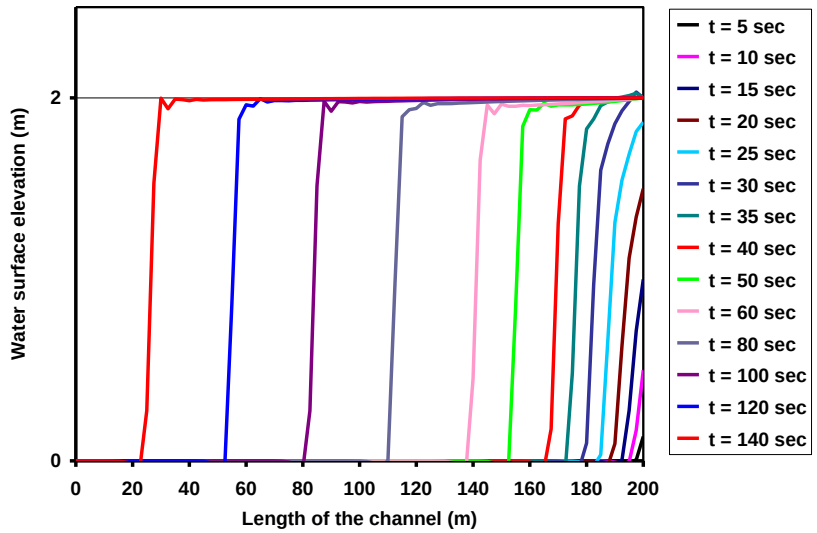

Figure 4. Water profiles along the channel due to bore propagation.

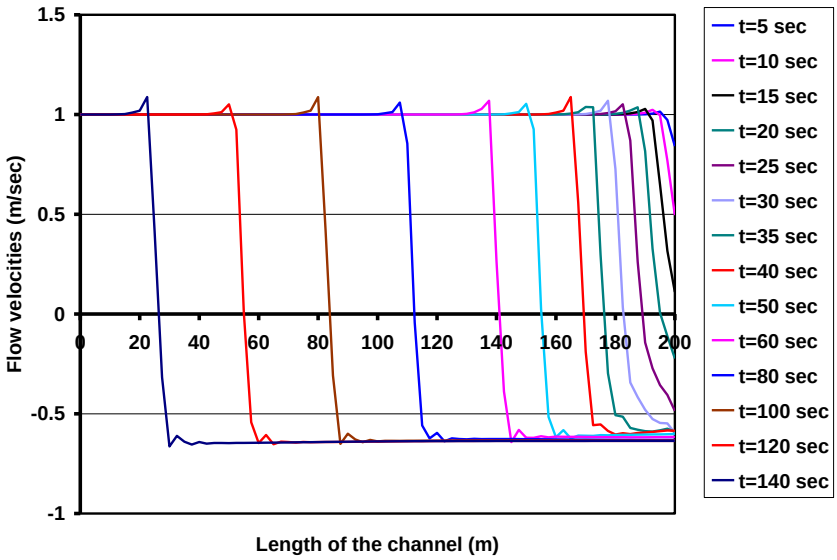

Figure 5. Flow velocities along the channel due to bore propagation.

4.2. Two-dimensional problems

A partial breaking of a dam over a wet bed which described in [9,30,32-34] is used to examine the shock capturing capability of the shallow water models. In this benchmark problem, the solution domain is a 200×200 m^2 flat rectangular domain with an asymmetric break. The whole domain is divided into 40×80 triangular elements with the same sizes. The dam thickness is 5 *m* in the direction of flow and the asymmetrical breaking part of dam has 75 m width. This breaking part is located in distance of 95 m from the right-hand side of the domain. Additional details of the domain are shown in Figure 6. The water depths inside the reservoir and in the tillage are 10 *m* and 5 *m*, respectively. By collapsing the dam, the water

moves toward the tillage. The flow field is computed numerically for 19 *sec* after the dam collapse. After breaking the dam, downstream traveling positive waves and upstream traveling negative waves are produced. The flow conditions were computed for t = 7.2 *sec* after the dam failure. At time t = 7.2 sec, the bore is well developed in the central portion of the tillage and the wave front has reached the left-hand bank of the domain.

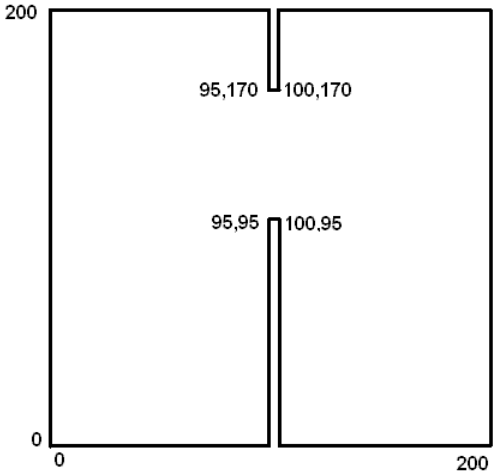

Figure 6. Geometry of the computational domain for partial dam-break.

Since no analytical solution is available for this problem, the results are compared with the reported ones by another numerical scheme in [32]. The numerical results is close to the results of aforementioned research. The results are presented in Figures 7 and 8 and compared with the solutions reported in [32]. In Figure 7, water surface elevations, presented as perspective plot of water surface, are compared with the result reported in [32]. The other comparison is carried out for water elevation contours in Figure 8. As shown in these Figures, the obtained results are in good agreement with those of previous works.

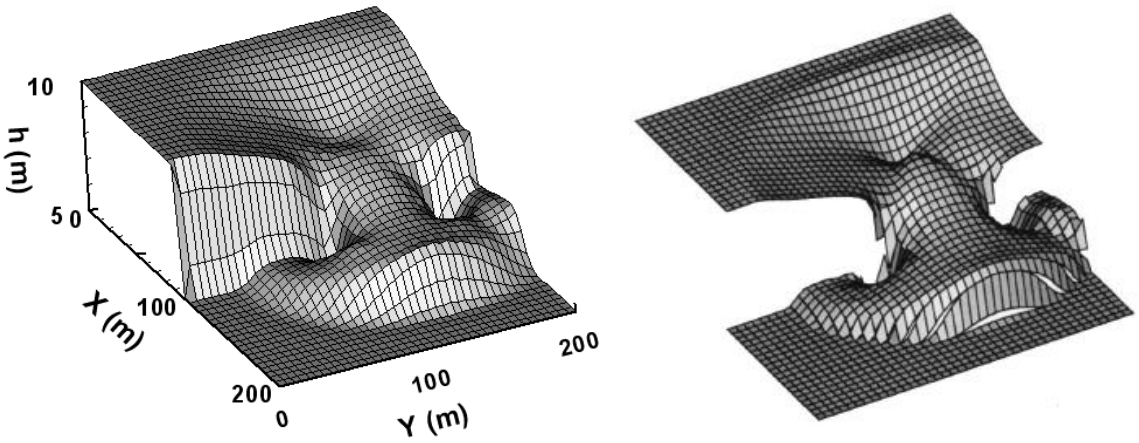

(a) **(b)**

Figure 7. Water surface profiles for partial dam-break at t = 7.2 *sec*

(a) Obtained by the model and (b) Reported in [32].

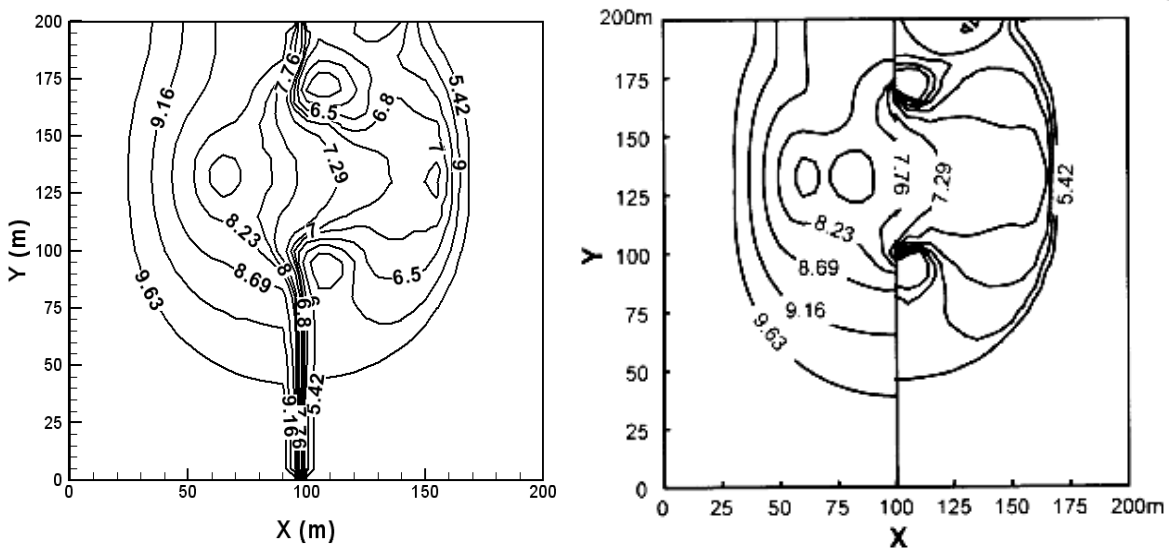

(a) **(b)**

Figure 8- Water elevation contours for partial dam-break at t = 7.2 *sec*

(a) obtained by the model and (b) reported in [32].

5. Conclusions

The CBS finite element model was presented for the solution of the two-dimensional dam-break problem. The described CBS finite element model has some significant features. Its stability is based on the flow velocity instead of the celerity which is especially useful for modeling the long term problems. The improved stability of the CBS algorithm along with its capability in simulating both sub- and super-critical flows are considered as main advantages of the method. Due to the highly non-linear nature of the dam-break problem, the model was verified using both one-dimensional and two-dimensional hypothetical dam-breaking. In spite of the high non-linearity in these problems, the comparison of the computational results with the analytical solutions and reported results of other numerical models, indicated the favorable performance of the used procedure in modeling the dam-break problems. As an important result, the described model can safely be used as an efficient tool for modeling other complicated free surface hydraulic problems. Based on the results of the presented test cases which indicated the high performance of the CBS finite element method, the model can be used for natural dam-break problems in different situations.

Acknowledgment

The author should like to thank Prof. Pablo Ortiz for his valuable helps on the CBS coding of shallow water equations. Also, special thanks to Dr. Mohammad H. Afshar for his useful helps and comments on the manuscript.

References

1. Wu G,Yang Zh, Zhang K, Dong P, Lin Y, (2018). A Non-Equilibrium Sediment Transport Model for Dam Break Flow over Moveable Bed Based on Non-Uniform Rectangular Mesh. Water, pp:10(5): 1-22.
2. Kocaman S, Ozmen-Cagatay H, (2015). Investigation of dam-break induced shock waves impact on a vertical wall. Journal of Hydrology, pp:525: 1–12.
3. Zheng XG, Pu JH, Chen RD, Liu XN, Shao SD, (2016). A Novel Explicit-Implicit Coupled Solution Method of SWE for Long-term River Meandering Process Induced by Dam break. Journal of Applied Fluid Mechanics, pp:9(6): 2647-2660.
4. Seyedashraf O, Mehrabi M, Akhtari AA, (2018). Novel approach for dam break flow modeling using computational intelligence. Journal of Hydrology, pp:559: 1028–1038.
5. Fang Q, Tang Ch, Chen Zh, Wang Sh, Yang T, (2019). A calculation method for predicting the run out volume of dam-break and non-dam-break debris flows in the Wenchuan earthquake area. Geomorphology, pp:327: 201–214.
6. Issakhov A, Zhandaulet Y, Nogaeva A, (2018). Numerical simulation of dam break flow for various forms of the obstacle by VOF method. International Journal of Multiphase Flow, pp:109 : 191–206.
7. Erpicum S, Dewals BJ, Archambeau P, Pirotton M, (2010). Dam break flow computation based on an efficient flux vector splitting. Journal of Computational and Applied Mathematics, pp:234: 2143–2151.
8. Sun X, Zhang J, Ren X, (2012). Characteristic-Based Split (CBS) Finite Element Method for Incompressible Viscous Flow with Moving Boundaries. Engineering Applications of Computational Fluid Mechanics, pp:6(3): 461-474.
9. Zoppou C, Roberts S, (2000). Numerical solution of the two-dimensional unsteady dam-break. Applied Mathematical Modeling, pp:24 (7):457-475.
10. Nithiarasu P, Zienkiewicz OC, (2000). On stabilization of the CBS algorithm: Internal and external time steps. International Journal for Numerical Methods in Engineering, pp:48:875-880.
11. Baggio, G. A. P., Silva, J. B. C. (2016). Tridimensional flow simulation with finite element stabilized by CBS scheme. Proceedings of the XXXVII Iberian Latin-American Congress on Computational Methods in Engineering, Brasília, DF, Brazil, November 6-9.
12. Douglas J, Russell TF, (1982). Numerical methods for convection-dominated diffusion problems based on combining the method of characteristics with finite element or finite difference procedures. SIAM Journal of Numerical Analysis, pp:19:871-885.

13. Jiang C, Zhang Z, Han X, Liu G, Lin T, (2018). A cell-based smoothed finite element method with semi-implicit CBS procedures for incompressible laminar viscous flows. International Journal for Numerical Methods in Fluids, pp:86:20-45.

14. Morandi-Cecchi M, Venturin M, (2006). Characteristic-based split (CBS) algorithm finite element modeling for shallow waters in the Venice lagoon. International Journal for Numerical Methods in Engineering, pp:66:1641-1657.

15. Ortiz P, (2012). Non-oscillatory continuous FEM for transport and shallow water flows. Computer Methods in Applied Mechanics and Engineering, pp:223:55–69.

16. Ortiz P, Zienkiewicz OC, Szmelter J, (2006). Hydrodynamics and transport in estuaries and rivers by the CBS finite element method. International Journal for Numerical Methods in Engineering, pp:66:1569-1586.

17. Ortiz, P., Zienkiewicz, O. C., Szmelter, J. (2004). CBS finite element modeling of shallow water and transport problems. European Congress on Computational Methods in Applied Sciences and Engineering, pp. 1–14.

18. Parsa, J., Afshar, M. H. (2006). CBS finite element model for shallow water problems. 7th International Conference on Coasts, Ports and Marine Structures, Book of abstract, pp. 32, Tehran, Iran, November 27-29.

19. Wang D, Tham LG, Shui Q, (2013). Dam-break model with Characteristic-Based Operator-Splitting Finite Element Method. Computer Modeling in Engineering and Science, pp:91(5):355-376.

20. Zienkiewicz OC, Nithiarasu P, Codina R, Vazquez M, Ortiz P, (1999). An efficient and accurate algorithm for fluid mechanics problems: The characteristic based split procedure. International Journal of Numerical Methods in Fluids, pp:31:359–392.

21. Zienkiewicz OC, Ortiz P, (1995). A split characteristic based finite element model for the shallow water equations. International Journal for Numerical Methods in Fluids, pp:20:1061–1080.

22. Zienkiewicz O.C., Taylor R.L., The finite element method: Volume 3: Fluid dynamics, Butterworth Heinemann, pp.218–228, 2000.

23. Chorin A, (1968). Numerical solution of the Navier Stokes equations. Mathematics of Computation, pp:22:745–762.

24. Daubert A, Graffe O, (1967) Quelques aspects des ecoulements presque horizontaux a deux dimensions en plan et nonpermanents aplication aux estuaries. La Houille Blanche, pp:8:847-860.

25. Verboom G., Stelling G., Officier M., Boundary conditions for the shallow water equations: Engineering Applications of Computational Hydraulics, Vol.1, Pitman, London, 1982.

26. Ortiz P, (2004). Finite elements using a plane wave basis for scattering of surface water waves. Philosophical Transactions of the Royal Society of London, Series A, pp:362:1-16.

27. Ortiz P, Sanchez E, (2001). Improved partition of unity finite element model for diffraction problems. International Journal for Numerical Methods in Engineering, pp:50:2727-2740.

28. Labadie G., Dalsecco S., Latteaux B., Resolution des equations de Saint Venant par une methode de elements finis, EDF Report HE/41/82, 1982.

29. Stoker J.J., Water waves: The mathematical theory with application, Interscience Publication, John Wiley & Sons, Inc., New York, 1957.

30. Alcrudo F, Garcia-Navarro P, (1993). A high-resolution Gudnov-type scheme in finite volumes for the 2-D shallow water equations. International Journal for Numerical Methods in Fluids, pp:16(6):489-505.

31. Hervouet J.M., Hydrodynamics of Free Surface Flows: Modelling with the Finite Element Method, Wiley, London, 2007.

32. Fagherazzi S, Rasetarinera P, Hussaini MY, Furbish DJ, (2004). Numerical solution of the dam-break problem with a discontinuous Galerkin method. Journal of Hydraulic Engineering, pp:130(6):532-539.

33. Fennema RJ, Chaudhry MH, (1990) Explicit methods for 2D transient free-surface flows. Journal of Hydraulic Engineering, pp:116(8):1013-1034.

34. Biscarini C, Francesco SDi, Manciola P, (2010). CFD modelling approach for dam break flow studies. Hydrology and Earth System Sciences, pp:14: 705–718.